SLAC–PUB–5657
September 1991
(E)

PRODUCTION OF THE $\rho_1(1300)$ IN THE REACTION $K^- P \rightarrow \pi^+\pi^-\Lambda$ AT 11 GeV/c*

D. Aston, T. Bienz, F. Bird, W. Dunwoodie, W. Johnson, P. Kunz, Y. Kwon, D. Leith, L. Levinson, B. Ratcliff, P. Rensing,[1] D. Schultz, S. Shapiro, P. Sinervo, G. Tarnopolsky, N. Toge, A. Waite, and S. Williams
Stanford Linear Accelerator Center
Stanford University, Stanford CA 94309, USA

N. Awaji, K. Fujii, H. Hayashii, S. Iwata, R. Kajikawa, T. Matsui, A. Miyamoto, H. Ozaki, C. Pak, T. Shimomura, A. Sugiyama, S. Suzuki, and T. Tauchi
Department of Physics
Nagoya University, Furo-cho, Chikusa-ku, Nagoya-shi 464, Japan

J. D'Amore, R. Endorf, J. Martinez, B. Meadows, and M. Nussbaum
Department of Physics
University of Cincinnati, Cincinnati, OH 45221, USA

K. Ukai
Institute for Nuclear Study
University of Tokyo, 3-2-1 Midori-cho, Tanashi-shi, Tokyo 188, Japan

ABSTRACT

Results are presented from an analysis of the forward $\pi^+\pi^-$ system produced in the reaction $K^-p \rightarrow \pi^+\pi^-\Lambda$ at 11 GeV/c observed with the LASS spectrometer at SLAC. An amplitude analysis reveals that the bump in the mass distribution in the vicinity of the $f_2(1270)$ actually contains a significant P-wave component. The mass dependence of the corresponding amplitude and phase is well described by a resonant Breit-Wigner line-shape with mass (1302^{+28}_{-25}) MeV/c^2, width (140^{+49}_{-40}) MeV/c^2, and estimated elasticity $\sim$ 5 %.

Presented at Particle and Fields '91, Vancouver, BC, Canada, August 18-22, 1991

*Work supported in part by Department of Energy contract DE–AC03–76SF00515, National Science Foundation grants PHY82–09144 and PHY85–13808, and the Japan–US Cooperative Research Project on High Energy Physics.

[1]Presented by P. Rensing.

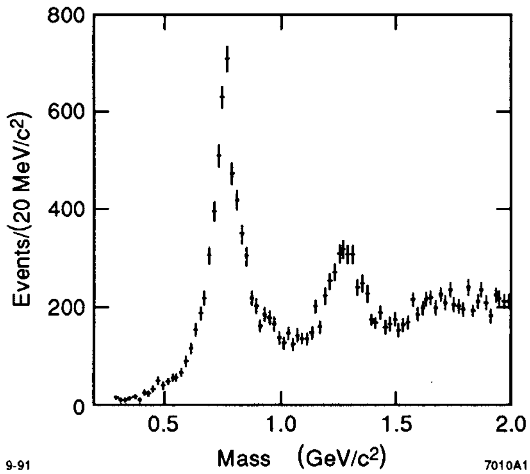

Fig. 1: The mass dependence of (a) the P_+ amplitude and (b) the $\pi^+\pi^-$ mass distribution for which $t_{\bar{p}\to\Lambda} \leq 2\,(\mathrm{GeV/c})^2$.

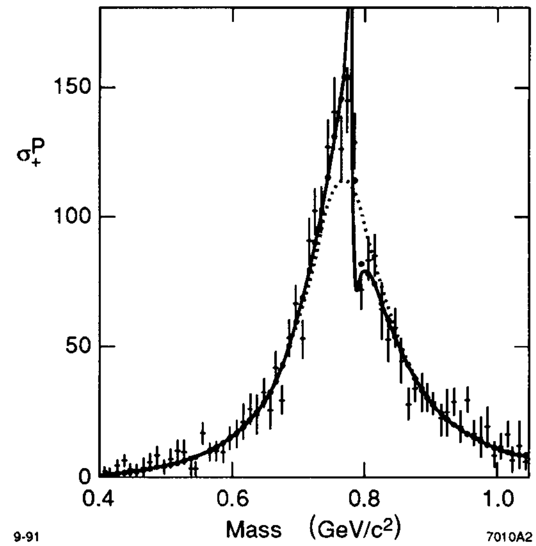

Fig. 2: The σ_+^P projection for the ρ region. See text for description.

1. The Data Sample

This paper presents results from an analysis of the forward $\pi^+\pi^-$ system observed in the reaction $K^-p \to \pi^+\pi^-\Lambda$ at an incident beam momentum of 11 GeV/c using the Large Aperture Superconducting Solenoid (LASS) spectrometer at SLAC. The spectrometer and relevant experimental details are described elsewhere.[1,2] The raw data sample represents an integrated luminosity of $4.1\,(\mathrm{nb})^{-1}$. The acceptance is approximately uniform over almost the full 4π solid angle.

Four-constraint fits to events of the two-prong V^0 topology yield $\sim$32,000 events corresponding to the reaction. In the forward sample, consisting of 26462 events, strong production of $\Sigma^+(1385)$ is observed in the $\Lambda\pi^+$ system, and there is clear evidence of the production of several higher mass Σ states in the mass range 1.7-2.1 GeV/c^2. The raw forward $\pi^+\pi^-$ mass distribution below 2 GeV/c^2 is shown in Fig. 1. Clear enhancements are observed for the $\pi^+\pi^-$ system in the vicinity of the $\rho(770)$ and $f_2(1270)$, and there is also some indication of structure around 1700 MeV/c^2.

In order to analyze the $\pi^+\pi^-$ system, the observed events are corrected for acceptance losses by weighting each event by the inverse of the acceptance function determined from Monte Carlo. The acceptance is only slowly varying, and the resulting spectrum is almost indistinguishable in shape from that of Fig. 1. To remove the overlap from Σ production, events having $m_{\Lambda\pi^+} < 2.1$ GeV/c^2 are removed from the data sample and, in each $\pi^+\pi^-$ mass bin, the spherical harmonic moments describing the

$\pi^+\pi^-$ angular distribution are corrected using the Monte Carlo data sample. A χ^2 minimization procedure is used to extract the underlying amplitudes which describe the $\pi^+\pi^-$ system.[3] See Ref. 4 for more details about the analysis and results.

2. $\rho - \omega$ Interference

In the ρ region, only S- and P-waves are required to describe the data, and the combination of moments,

$$\sigma_+^P \equiv \frac{1}{3}\, t_{00} - \frac{\sqrt{5}}{6}\, t_{22} - \sqrt{\frac{5}{6}}\, t_{22} = |P_+|^2 + |S|^2/3 \tag{1}$$

which projects the P-wave natural parity exchange cross section yields the mass distribution shown in Fig. 2. The S-wave contribution is negligible compared to that due to P_+.

The distribution of Fig. 2 cannot be described well by a single Breit-Wigner line-shape (the dotted curve), and shows clear evidence of ρ–ω interference. The distribution is fit to the line-shape which incorporates ρ–ω mixing to all orders, but which assumes that the transition element $T(\omega \to \pi^+\pi^-)$ is zero.[4,5] The parameters of the ρ and ω were fixed to the PDG values.[6] The solid curve in Fig. 2 shows the fitted function while the star points represent the function smeared by the resolution and integrated over the bins. The fit yields the value (2.15 ± 0.35) MeV/c^2 for the ρ–ω mass-mixing term and (-8 ± 10) degrees for the relative phase. Assuming equal and coherent ρ and ω production amplitudes, this implies a branching fraction of $(1.5 \pm 0.5)\%$ for the decay $\omega \to \pi^+\pi^-$, in good agreement with the original estimates[7–9] and with the present world average.[6]

3. The Amplitude Analysis in the Vicinity of the $f_2(1270)$

The amplitude analysis described in Sec. 1 was carried out using S-, and P-waves (ie., six parameters) in the mass region up to 1.0 GeV/c^2 and using S-, P- and D-waves (12 parameters) from 1.0 GeV/c^2 to 1.5 GeV/c^2. The data points are the average of any multiple solutions, and the errors are found by searching the χ^2 function. In the ρ region, the P_+ amplitude has the ρ–ω mixing structure discussed in Sec. 2; however, at higher mass the amplitude does not simply decrease as the tail of the ρ Breit-Wigner, but shows a second maximum at ~ 1.28 GeV/c^2. This bump agrees quite well with a P-wave Breit-Wigner of mass ~ 1.29 GeV/c^2, but the errors are large, due mostly to multiple solutions to the amplitude analysis. In order to better define the P-wave amplitude, the D_+ amplitude was set to the $f_2(1270)$ Breit-Wigner shape with fixed amplitude. The amplitude analysis was redone using S-, P- and D-waves up to 1.5 GeV/c^2. The P_+ amplitude and the P_+-D_+ relative phase are fitted with two Breit-Wigners; the result is shown in Fig. 3. This fit yields mass and width values of (1302^{+28}_{-25}) MeV/c^2 and (140^{+48}_{-40}) MeV/c^2, respectively, for this new state, the $\rho_1(1300)$. The $\rho_1(1300)$ phase is 102 ± 24 degrees and the P_+–D_+ phase is 3 ± 10 degrees. The resulting description of the data of Fig. 3(b) is clearly very good. The dotted curves of Fig. 3 correspond to

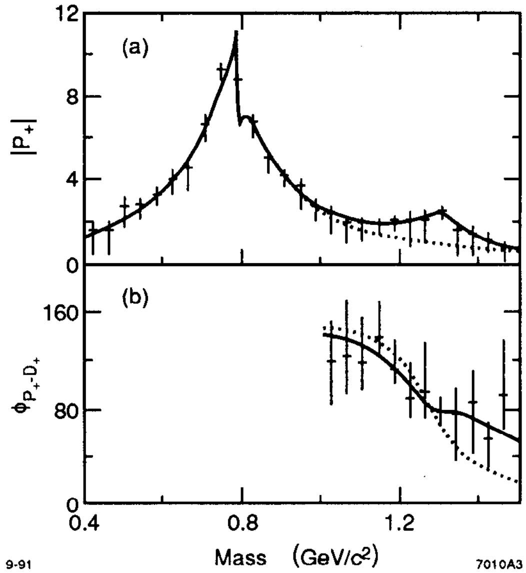

Fig. 3: The mass dependence of (a) the P_+ amplitude and (b) the P_+–D_+ phase resulting from the fit to the moments with the D_+ amplitude fixed.

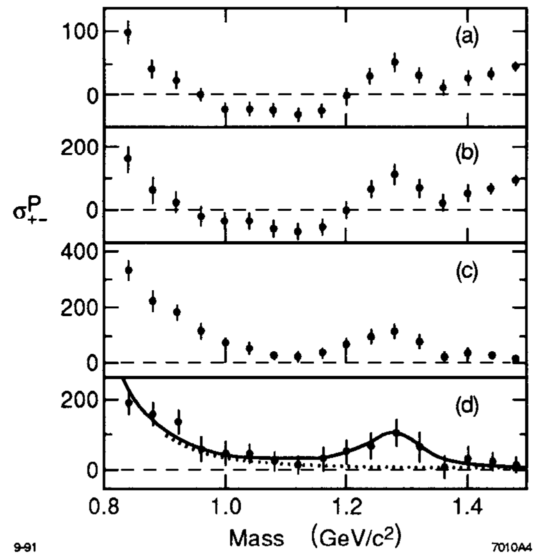

Fig. 4: The σ^P_{+-} projection of the data at different stages of the analysis. See text for description.

no $\rho_1(1300)$ contribution, and do not provide a good description of the data. Finally, the size of the $\rho_1(1300)$ amplitude relative to that of the $\rho(770)$ indicates an elasticity $\sim 5\%$ for this state.

As further evidence for the $\rho_1(1300)$, Fig. 4 shows the progression of the combination of moments

$$\sigma^P_{+-} \equiv \sqrt{\frac{5}{2}}\, t_{42} - \sqrt{\frac{10}{3}}\, t_{22} = |P_+|^2 - |P_-|^2 \tag{2}$$

in the absence of significant F-wave, through the different stages of the analysis. Figure 4(a) shows σ^P_{+-} for the raw data sample; Fig. 4(b) for the acceptance corrected data; Fig. 4(c) for the data with the Σ overlap removed; and Fig. 4(d) for the data corrected for the Σ removal. The bump in the P-wave around 1.28 GeV/c^2 is clearly visible in all cases, indicating that it is very unlikely to be a figment of the analysis, instead of a feature of the data. A curve corresponding to the $\rho_1(1300)$ is drawn on Fig. 4(d) to show the agreement.

The present result agrees in some respects with the analysis of Donnachie and Mirzaie,[10] namely the elasticity and approximate width, but is significantly lower in mass. Part of the difference arises from the treatment of the ρ_1 phase; this analysis allows the phase to vary, while in Ref. 10 it is fixed to 180 degrees, which is in disagreement with the present result. More data are needed to resolve the disagreement.

4. Conclusion

The present analysis of the forward $\pi^+\pi^-$ system in reaction (1) has revealed a rather striking corroboration of the phenomenon of ρ–ω interference. The resulting value of the $\omega \rightarrow \pi^+\pi^-$ branching fraction, $(1.5 \pm 0.5)\,\%$, agrees well with the present world average, and also with theoretical expectations. An amplitude analysis of the spherical harmonic moments describing the $\pi^+\pi^-$ angular distribution has provided evidence for the existence of a new P-wave state, the $\rho_1(1300)$. The $\rho_1(1300)$ mass and width were found to be (1302^{+28}_{-25}) MeV/c^2 and (140^{+48}_{-40}) MeV/c^2, respectively; this state has elasticity $\sim 5\%$, and is most readily understood as the first radial excitation of the $\rho(770)$.

Reference

1. D. Aston et al., *The LASS Spectrometer,* SLAC–REP–298 (1986).
2. D. Aston et al., Nucl. Phys. **B301**, 525 (1988).
3. See for example, A. Martin et al., Nucl. Phys. **B140**, 158 (1978).
4. D. Aston et al., SLAC–PUB–5606, to be published.
5. G. Goldhaber, "Experimental Results on the ω–ρ Interference Effect," in *Experimental Meson Spectroscopy* (Columbia University Press, New York, 1970), p. 59 *et seq.*
6. Particle Data Group, Phys. Lett. **239B** (1990).
7. S.L. Glashow, Phys. Rev. Lett. **7**, 469 (1961).
8. S. Coleman and S.L. Glashow, Phys. Rev. **134B** 671 (1964).
9. S. Coleman et al., "Electromagnetic Mass Differences of Strongly Interacting Particles," in *Proc. XII Int. Conf. on High Energy Physics, Dubna, 1964* (Atomizdat, Moscow, 1966) Vol. 1, pp. 785–787.
10. A. Donnachie and H. Mirzaie, Zeit. Phys. **C33**, 407 (1987).